*Inorg. Chem.* **2007**, *46*, 2864–2869

# Iodination of Stanna-*closo*-dodecaborate

**Torben Gädt,[†] Falko M. Schappacher,[§] Rainer Pöttgen,[§] and Lars Wesemann*,[†]**

*Institut für Anorganische Chemie, Universität Tübingen, Auf der Morgenstelle 18, D-72076 Tübingen, Germany, and Institut für Anorganische und Analytische Chemie, Universität Münster, Corrensstrasse 30, D-48149 Münster, Germany*

Received December 1, 2006

The dianionic stannaborate $[SnB_{11}H_{11}]^{2-}$ oxidatively adds iodine at the tin vertex to give the iodinated cluster $[I_2SnB_{11}H_{11}]^{2-}$ which maintains a closo structure, albeit having a nido electron count. The iodo-stannaborate $[I_2SnB_{11}H_{11}]^{2-}$ is unstable at room temperature, but its structure was elucidated via single-crystal X-ray diffraction at low temperatures. The low-temperature $^{11}B$ NMR spectrum exhibits a 5:1:5 signal pattern, and the $^{119}Sn$ NMR shows a resonance at −1039 ppm. Iodination of the zwitterionic stannaborate iron complex $Fe(SnB_{11}H_{11})$(triphos) leads to the formation of the corresponding iodo-stannaborate iron complex $Fe(I_2SnB_{11}H_{11})$(triphos) which features an iodinated stannaborate moiety that has a structure analogous to that of $[I_2SnB_{11}H_{11}]^{2-}$. The zwitterionic iodo-stannaborate complex is stable at room temperature, and the crystal structure and the $^1H$, $^{11}B$, $^{31}P$, and $^{119}Sn$ NMR parameters were determined. $^{119}Sn$ Mössbauer spectroscopy supports the assignment of a tin oxidation state of +II for $Fe(SnB_{11}H_{11})$(triphos) ($\delta = 2.71$ mm s$^{-1}$) and +IV for $Fe(I_2SnB_{11}H_{11})$(triphos) ($\delta = 1.22$ mm s$^{-1}$). Additional $^{57}Fe$ Mössbauer spectra confirm the iron oxidation state +II for both compounds.

## Introduction

The structures and electron-counting rules of simple polyhedral borane clusters are covered in contemporary inorganic chemistry textbooks. The seminal contributions of Williams,[1] Wade,[2] and Rudolph[3] established the systematics of the structure patterns of these systems and elucidated the corresponding electron-counting rules. These electron-counting rules are applicable to metal clusters: this was also recognized by Mingos.[4,5] The appeal of the Wade rules derives from their simplicity and their success in explaining the majority of cluster structures. Reported exceptions are of considerable interest because they help to clarify the limitations of the concept and potentially facilitate the recognition of new patterns. Metallaboranes constitute the largest group of structurally characterized examples which deviate from Wade's rules.[6] Recent work by Fehlner and co-workers for example lead to the isolation of a series of hypoelectronic rhenaboranes which exhibit noncanonical deltahedral structures in terms of the Wade rules.[7,8] The number of main group heteroboranes which do not obey the Wade rules is much smaller than the number of disobedient heteroboranes with transition metal vertices.[9] It is therefore of particular interest to obtain more experimental findings for non-Wadian main group heteroborane clusters.

As part of our investigations of the chemistry of the dianionic stanna-*closo*-dodecaborate cluster $[SnB_{11}H_{11}]^{2-}$, we became interested in the reaction with main group electrophiles. It is well documented that $[SnB_{11}H_{11}]^{2-}$ has nucleophilic properties and is a versatile ligand in the coordination chemistry of transition metals.[10−13] We present here our results for the oxidative addition of iodine to the stannaborate cluster.

## Results and Discussion

**Synthesis.** When a dichloromethane solution of iodine is added dropwise to a solution of $[Bu_3MeN]_2[SnB_{11}H_{11}]$, the

* To whom correspondence should be addressed. Email: lars.wesemann@uni-tuebingen.de.
[†] Universität Tübingen.
[§] Universität Münster.

(1) Williams, R. E. *Adv. Inorg. Chem. Radiochem.* **1976**, *18*, 67−142.
(2) Wade, K. *Adv. Inorg. Chem. Radiochem.* **1976**, *18*, 1−66.
(3) Rudolph, R. W. *Acc. Chem. Res.* **1976**, *9*, 446−452.
(4) Mingos, D. M. P. *Nat. Phys. Sci.* **1972**, *236*, 99−102.
(5) Mingos, D. M. P.; Johnston, R. L. *Struct. Bonding* **1987**, *68*, 29−87.
(6) Kennedy, J. D. Disobedient Skeletons. In *The Borane, Carborane, Carbocation Continuum*; Casanova, J., Ed.; John Wiley & Sons: New York, 1998; pp 85−116 and references cited therein.
(7) Wadepohl, H. *Angew. Chem.* **2002**, *114*, 4394−4397.
(8) Guennic, B. L.; Jiao, H.; Kahlal, S.; Saillard, J.-Y.; Halet, J.-F.; Ghosh, S.; Shang, M.; Beatty, A. M.; Rheingold, A. L.; Fehlner, T. P. *J. Am. Chem. Soc.* **2004**, *126*, 3203−3217.
(9) Wesemann, L.; Ramjoie, Y.; Trinkaus, M.; Ganter, B.; Müller, J. *Angew. Chem., Int. Ed.* **1998**, *37*, 1412−1415; *Angew. Chem.* **1998**, *110*, 1481−1484.



10.1021/ic0622858 CCC: $37.00 
Published on Web 02/21/2007

**Scheme 1.** Synthesis of $[I_2SnB_{11}H_{11}]^{2-}$

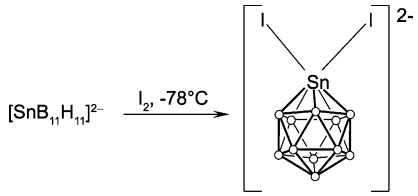


**1**

color of the reaction mixture becomes orange-red immediately because of the formation of the iodinated product $[Bu_3MeN]_2[I_2SnB_{11}H_{11}]$ (**1**) (Scheme 1). However, at room temperature under argon atmosphere, the color of the reaction mixture disappears within hours indicating the instability of **1** at ambient temperature. If the reaction is conducted at −78 °C and the reaction mixture is subsequently stored at −30 °C, the red color of the solution persists for weeks.

Because of the instability of **1** at room temperature, it is desirable to prepare a stable iodinated stannaborate derivative. We thus treated a dichloromethane solution of the recently described[13] zwitterionic iron stannaborate complex Fe(SnB$_{11}$H$_{11}$)(triphos) (**2**) (triphos = 1,1,1-tris(diphenylphosphanylmethyl)ethane) with iodine. In fact, Fe(I$_2$SnB$_{11}$H$_{11}$)(triphos) (**3**) forms as a brown precipitate 5 min after the addition of iodine (Scheme 2). The solid is isolated via filtration and can be redissolved in DMSO only.

**Solid-State Structure.** The layering of the red dichloromethane solution of **1** with hexane in a Schlenk tube, which is kept at −30 °C, yields a red crystalline material. The red crystals decompose rapidly when exposed to air. Fortunately, a single-crystal structure analysis was possible nonetheless. The molecular structure of the anion of $[Bu_3MeN]_2[I_2SnB_{11}H_{11}]$ is depicted in Figure 1. A striking feature is the two-fold coordination of the tin vertex with two iodine atoms. The Sn−I distances are Sn−I(1) = 2.797(1) Å and Sn−I(2) = 2.862(1) Å. and the I−Sn−I angle is to 86.08(2)°. The Sn−I separations are somewhat longer than in $SnI_4$ (2.658 and 2.662 Å),[14] but they are of similar magnitude compared to the Sn−I separations in other Sn(IV) compounds such as (nacnac)$SnI_3$ (Sn−I = 2.790 Å; nacnac = (2,6-$^i$Pr$_2$C$_6$H$_3$)NC(Me)C(H)C(Me)N(2,6-$^i$Pr$_2$C$_6$H$_3$)).[15] The tin vertex is located above the center of the pentagonal $B_5$ face, and all Sn−B distances are similar ranging from 2.299(9) to 2.335(8) Å with an average value of 2.314 Å, which is similar to the tin boron separation in transition metal coordination compounds of $[SnB_{11}H_{11}]^{2-}$.[16] It can thus be concluded that the tin vertex is not slipped. Moreover, it is noteworthy that

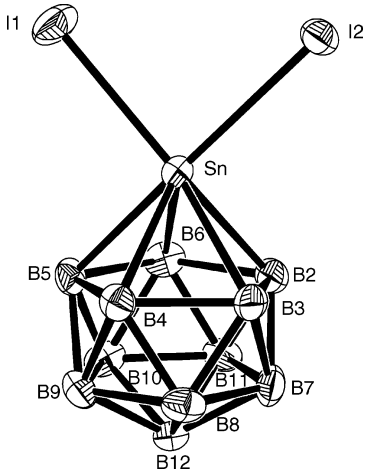


**Figure 1.** ORTEP plot (50% probability level) of the molecular structure of $[Bu_3MeN]_2[I_2SnB_{11}H_{11}]$ (**1**). The hydrogen atoms have been omitted for clarity. Selected bond distances (Å) and angles (deg): B(2)−Sn = 2.317(9), B(3)−Sn = 2.317(9), B(4)−Sn = 2.304(8), B(5)−Sn = 2.335(8), B(6)−Sn = 2.299(9), I(1)−Sn = 2.797(1), I(2)−Sn = 2.862(1), I(1)−I(2) = 3.862(1); B(2)−Sn−I(1) = 158.0(3), B(3)−Sn−I(1) = 154.1(3), B(4)−Sn−I(1) = 112.0(2), B(5)−Sn−I(1) = 94.7(2), B(6)−Sn−I(1) = 114.6(3), B(2)−Sn−I(2) = 95.5(2), B(3)−Sn−I(2) = 98.3(2), B(4)−Sn−I(2) = 135.2(2), B(5)−Sn−I(2) = 176.2(2), B(6)−Sn−I(2) = 128.5(3), I(1)−Sn−I(2) = 86.08(2).

B(5)−Sn (2.335(8) Å) is the longest B−Sn edge and lies directly opposite to the Sn−I(1) bond with a B(5)−Sn−I(2) angle of 176.2(2)°. The structural data leave no doubt that the heteroborate maintains a closo structure.

Dark brown-red crystalline material of **3** can be obtained by layering an acetonitrile solution of **2** with a diethylether solution of $I_2$. The molecular structure, together with selected interatomic angles and distances, is depicted in Figure 2. The tin atom is coordinated with two iodine atoms with interatomic distances of I(1)−Sn = 2.788(1) Å and I(2)−Sn = 2.760(1) Å, which are slightly shorter than those of **1**. The I−Sn−I angle is 90.27(1)° and thus is approximately 4° larger than that of **1**. Furthermore, the tin boron separations exhibit a relatively large variation with values between 2.288(4) Å for B(2)−Sn and the equally long edges B(3)−Sn (2.391(5) Å) and B(6)−Sn (2.394(4) Å). The average value is 2.352 Å. The shortest value for B(2)−Sn is consistent with the findings for recently reported derivatives of **2**,[13] and the longer Sn−B edges correspond to edges which are approximately opposite to the iodine−tin bond with a B(3)−Sn−I(2) angle of 171.02(11)° and a B(6)−Sn−I(1) angle of 166.32(10)°.

**NMR Spectroscopy.** The $^{11}$B{$^1$H} NMR spectrum (measured at −30 °C) of **1** exhibits three signals at −15.3, −17.2, and −18.2 ppm with an intensity ratio of 5:1:5. The $^{11}$B−$^{11}$B COSY spectrum allows unambigous assignment of the signal at −15.3 ppm to the first $B_5$ belt (B2−B6) and the signal at −18.2 ppm to the second $B_5$ belt (B7−B11), while the antipodal boron vertex B12 can be assigned to the resonance at −17.2 ppm. The free stannaborate cluster, the alkylated and arylated stannaborate derivatives [1-R-SnB$_{11}$H$_{11}$]$^-$ (R = alkyl, aryl),[17,18] and the $\eta^1$(Sn)-coordinated

(10) Hagen, S.; Pantenburg, I.; Weigend, F.; Wickleder, C.; Wesemann, L. *Angew. Chem., Int. Ed.* **2003**, *42*, 1501−1505; *Angew. Chem.* **2003**, *115*, 1539−1543.
(11) Marx, T.; Mosel, B.; Pantenburg, I.; Hagen, S.; Schulze, H.; Wesemann, L. *Chem.−Eur. J.* **2003**, *9*, 4472−4478.
(12) Hagen, S.; Wesemann, L.; Pantenburg, I. *Chem. Commun.* **2005**, 1013−1015.
(13) Gädt, T.; Eichele, K.; Wesemann, L. *Organometallics* **2006**, *25*, 3904−3911.
(14) Reuter, H.; Pawlak, R. *Z. Kristallogr.* **2001**, *216*, 34−38.
(15) Räke, B.; Zülch, F.; Ding, Y.; Prust, J.; Roesky, H. W.; Noltemeyer, M.; Schmidt, H. G. *Z. Anorg. Allg. Chem.* **2001**, *627*, 836−840.
(16) Wesemann, L.; Marx, T.; Englert, U.; Ruck, M. *Eur. J. Inorg. Chem.* **1999**, 1563−1566.
(17) Chapman, R. W.; Kester, J. G.; Folting, K.; Streib, W. E.; Todd, L. J. *Inorg. Chem.* **1992**, *31*, 979−983.

**Scheme 2.** Synthesis of $Fe(I_2SnB_{11}H_{11})$(triphos) (**3**)

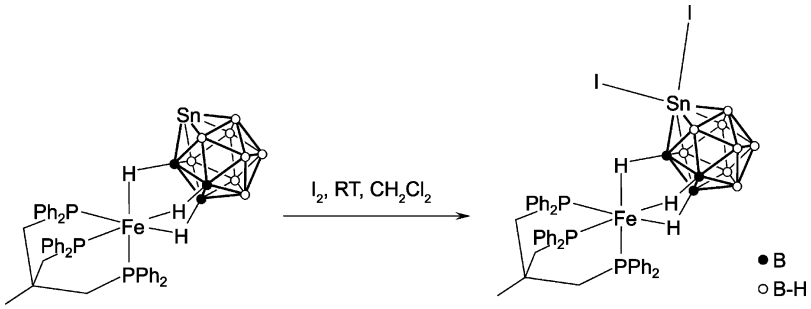


**2** **3**

transition metal complexes of $[SnB_{11}H_{11}]^{2-}$ have in common that the antipodal boron vertex is the most high-frequency-shifted boron vertex. It is therefore noteworthy that the $^{11}B$ signal pattern of alkylated stannaborates and the tin−metal-bonded complexes is usually 1:10, which is significantly different from that of the iodinated stannaborate cluster which exhibits a 5:1:5 pattern. Furthermore, the $C_s$ symmetry of the iodinated stannaborate cluster in the solid state should give rise to seven signals in the $^{11}B\{^1H\}$ NMR spectrum. The occurrence of three signals in solution corresponds to an effective $C_{5v}$ symmetry of **1** and can be compared with the $^{11}B\{^1H\}$ NMR spectrum of $[(Ph_3P)_2RhB_{11}H_{11}]^{3-}$.[19] The higher effective symmetry in solution could be explained by a small rotational barrier of the $SnI_2$ fragment on the $B_{11}H_{11}$ ligand. Rotational barriers for complexes with carbaboranes were studied by $^{31}P$ NMR spectroscopy and theoretical calculations for $[1,1\text{-}(Et_3P)_2\text{-}1,2,4\text{-}PtC_2B_9H_{11}]$ and $[1,2\text{-}(Et_3P)_2\text{-}2,4\text{-}Me_2\text{-}1,2,4\text{-}PtC_2B_4H_4]$.[20] The $^{119}Sn\{^1H\}$ NMR spectrum (measured at −30°) displays a resonance at −1039 ppm which is the most low-frequency-shifted value reported so far for stannaborate derivatives. The large shift is plausible because iodine ligands are known to cause large low-frequency shifts in $^{119}Sn\{^1H\}$ NMR spectroscopy.[21]

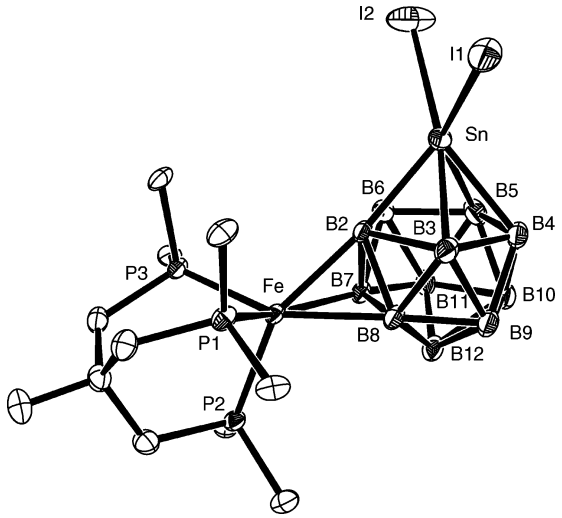


**Figure 2.** ORTEP plot (50% probability level) of the molecular structure of $Fe(I_2SnB_{11}H_{11})$(triphos) (**3**). The hydrogen atoms and phenyl rings except for the *ipso*-carbon atoms have been omitted for clarity. Selected bond distances (Å) and angles (deg): B(2)−Sn = 2.288(4), B(3)−Sn = 2.391(5), B(4)−Sn = 2.336(5), B(5)−Sn = 2.350(5), B(6)−Sn = 2.394(4), B(2)−Fe = 2.272(4), B(7)−Fe = 2.227(4), B(8)−Fe = 2.245(4), I(1)−Sn = 2.788(1), I(2)−Sn = 2.760(1), Fe−P(1) = 2.227(1), Fe−P(2) = 2.220(1), Fe−P(3) = 2.218(1); I(2)−Sn−I(1) = 90.27(1), B(2)−Sn−I(2) = 124.25(10), B(3)−Sn−I(2) = 171.02(11), B(4)−Sn−I(2) = 141.89(13), B(5)−Sn−I(2) = 102.59(13), B(6)−Sn−I(2) = 94.58(11), B(2)−Sn−I(1) = 120.17(10), B(3)−Sn−I(1) = 91.60(10), B(4)−Sn−I(1) = 103.60(11), B(5)−Sn−I(1) = 145.55(12), B(6)−Sn−I(1) = 166.32(10), P(1)−Fe−P(2) = 91.31(4), P(1)−Fe−P(3) = 89.93(4), P(2)−Fe−P(3) = 89.56(4).

The $^1H$ NMR and $^{31}P\{^1H\}$ NMR spectra of **3** confirm that the $\eta^3$(B−H) coordination of the exo polyhedral iron fragment remains intact in solution. Two broad signals in the $^1H$ NMR spectrum at −10.58 and −10.94 ppm with an integration ratio of 1:2 can be attributed to the hydridic B−H−Fe protons. The phosphorus NMR spectrum exhibits an $A_2B$ pattern with chemical shifts of $\delta_A = 51.2$ ppm and $\delta_B = 53.2$ ppm and a coupling constant of $^2J(^{31}P, ^{31}P) = 55.7$ Hz, which is similar to the values described for related systems.[13] As expected, the influence of the iodine atoms is reflected in the $^{11}B\{^1H\}$ NMR spectrum which displays two moderately broad resonances at −31.0 and −38.7 ppm and extremely broad, unresolved resonances between −13.0 and −25.0 ppm. The signals at −31.0 and −38.7 ppm have an integration ratio of 2:1, and the signal at −31.0 ppm can therefore be attributed to the B−H vertices of the second $B_5$ belt, which are coordinated to the iron fragment, while the signal at −38.7 ppm belongs to B(2). The $^{119}Sn\{^1H\}$ NMR spectrum shows a broad resonance at −749 ppm which is low-frequency shifted compared to **2** (−623 ppm) but high-frequency shifted compared to **1** (−1039 ppm).

**$^{57}$Fe and $^{119}$Sn Mössbauer Spectroscopy.** $^{119}Sn$ and $^{57}Fe$ Mössbauer spectra recorded at 78 K of **2** and **3** are presented in Figures 3 and 4, together with transmission integral fits. The corresponding fitting parameters are listed in Table 2. The spectrum of $Fe(I_2SnB_{11}H_{11})$(triphos) was well reproduced with a single tin site at an isomer shift of 1.22(1) mm/s, compatible with tetravalent tin.[22] The signal shows only weak quadrupole splitting of 0.20(2) mm/s. For a reasonable fit of the $Fe(SnB_{11}H_{11})$(triphos) spectrum, two additional contributions (not listed with the main signals in Table 2) have been accounted for in the fit. One small contribution at $\delta =$ 0.07 mm/s can be attributed to a small $SnO_2$ impurity,[22] while the nature of the second small contribution around $\delta = 1.84$ mm/s is unknown. The much larger isomer shift of **2** of 2.71-

(18) Ronig, B.; Bick, T.; Pantenburg, I.; Wesemann, L. *Eur. J. Inorg. Chem.* **2004**, 689−693.
(19) Dirk, W.; Paetzold, P. *Z. Anorg. Allg. Chem.* **2001**, *627*, 2615−2618.
(20) (a) Barker, G. K.; Green, M.; Stone, F. G. A.; Welch, A. J. *J. Chem. Soc., Dalton Trans.* **1980**, 1186−1199. (b) Calhorda, M. J.; Mingos, D. M. P.; Welch, A. J. *J. Organomet. Chem.* **1982**, *228*, 309−320.
(21) Wrackmeyer, B. *Annu. Rep. NMR Spectrosc.* **1985**, *16*, 73−186.
(22) Lippens, P. E. *Phys. Rev. B* **1999**, *60*, 4576−4586.

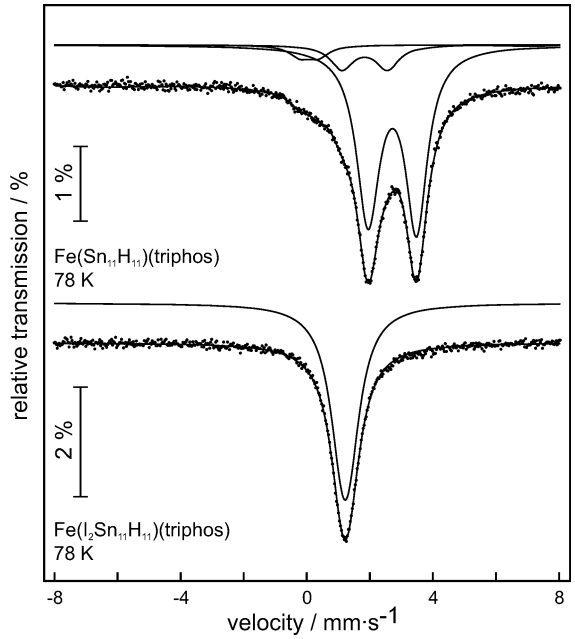


**Figure 3.** Experimental and simulated $^{119}$Sn Mössbauer spectra of Fe($Sn_{11}H_{11}$)(triphos) and Fe($I_2Sn_{11}H_{11}$)(triphos) at 78 K.

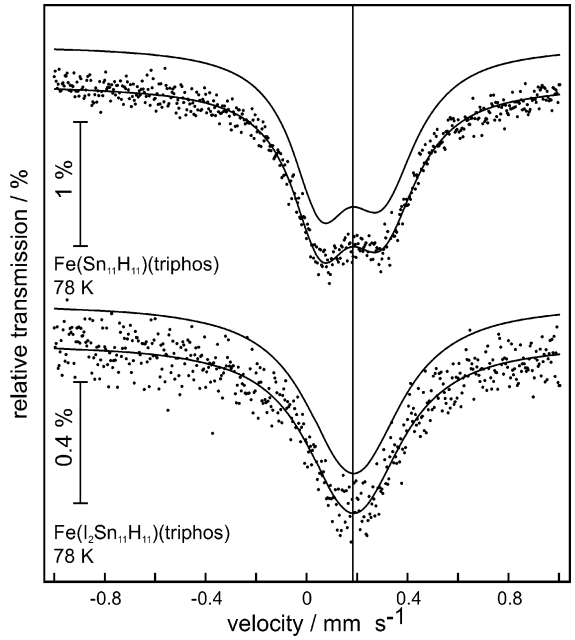


**Figure 4.** Experimental and simulated $^{57}$Fe Mössbauer spectra of Fe($Sn_{11}H_{11}$)(triphos) and Fe($I_2Sn_{11}H_{11}$)(triphos) at 78 K.

(1) mm/s is compatible with divalent tin. The $^{119}$Sn spectra thus nicely reflect the oxidation of divalent tin in Fe($SnB_{11}H_{11}$)(triphos) by iodine to tetravalent tin in Fe($I_2$-$SnB_{11}H_{11}$)(triphos). It is worthwhile to note that **2** shows a much higher electric quadrupole splitting parameter (1.54-(1) mm/s). This is tentatively attributed to the influence of the lone pair at the tin vertex which is missing in compound **3**. It is instructive to note that the methylated stannaborate $[MeSnB_{11}H_{11}]^-$ has a quadrupole splitting of 0.95 mm/s and the square-planar complex $[Pt(SnB_{11}H_{11})_4]^{6-}$ exhibits a value of $\Delta E_Q = 1.51$ mm/s.[11] Obviously, the coordination geometry around the tin vertex must also be considered to account for the observed trends in the quadrupole splitting.

**Table 1.** Crystal Data and Data Collection and Refinement Parameters for Compounds **1** and **3**

| | **1** | **3** |
|---|---|---|
| formula | $C_{26}H_{71}B_{11}I_2N_2Sn$ | $C_{45}H_{56}B_{11}FeI_2N_2P_3Sn$ |
| $M$ | 903.25 | 1265.08 |
| temp (K) | 173(2) | 173(2) |
| system | triclinic | triclinic |
| space group | $P\bar{1}$ | $P\bar{1}$ |
| $a$ (Å) | 10.2058(8) | 11.5022(9) |
| $b$ (Å) | 11.5017(11) | 12.1020(9) |
| $c$ (Å) | 19.2119(17) | 19.9242(14) |
| $\alpha$ (deg) | 78.689(7) | 87.162(6) |
| $\beta$ (deg) | 76.260(7) | 86.792(6) |
| $\gamma$ (deg) | 72.300(7) | 81.350(6) |
| $V$ (Å$^3$) | 2068.1(3) | 2735.2(4) |
| $Z$ | 2 | 2 |
| $d_{calcd}$ (g cm$^{-1}$) | 1.450 | 1.536 |
| $\mu$ (mm$^{-1}$) | 2.130 | 1.971 |
| $F$(000) | 904 | 1244 |
| $\theta_{max}$ (deg) | 29.38 | 26.85 |
| reflns | 29 511 | 40 577 |
| indep obsd reflns | 10 978 | 11 626 |
| $T_{max}$, $T_{min}$ | 0.8002, 0.6217 | 0.7989, 0.5261 |
| params | 368 | 632 |
| GOF | 1.102 | 1.105 |
| $R_1$ (obsd data) | 0.0727 | 0.0437 |
| $R_2$ (obsd data) | 0.1826 | 0.1036 |
| res el dens (e Å$^{-3}$) | 2.377, −1.580 | 2.107, −1.973 |

**Table 2.** Fitting Parameters of $^{57}$Fe and $^{119}$Sn Mössbauer Measurements for Fe($SnB_{11}H_{11}$)(triphos) and Fe($I_2SnB_{11}H_{11}$)(triphos)[a]

| compound | $\delta$ (mm /s) | $\Gamma$ (mm/s) | $\Delta E_Q$ (mm/s) | $\chi^2$ |
|---|---|---|---|---|
| | $^{57}$Fe data at 78 K | | | |
| Fe($SnB_{11}H_{11}$)(triphos) | 0.18(1) | 0.27(1) | 0.24(1) | 1.04 |
| Fe($I_2SnB_{11}H_{11}$)(triphos) | 0.16(22) | 0.36(43) | 0.10(17) | 1.04 |
| | $^{119}$Sn data at 78 K | | | |
| Fe($SnB_{11}H_{11}$)(triphos) | 2.71(1) | 0.89(2) | 1.54(1) | 1.03 |
| Fe($I_2SnB_{11}H_{11}$)(triphos) | 1.22(1) | 0.95(1) | 0.20(2) | 1.06 |

[a] Numbers in parentheses represent the statistical errors in the last digit. $\delta$ = isomer shift, $\Gamma$ = experimental line width, and $\Delta E_Q$ = electric quadrupole splitting. All the parameters are in units of mm/s ($\chi^2$ is a fit quality factor).

The $^{57}$Fe spectra show an almost similar isomer shift (Table 2) but, again, with a larger quadrupole splitting parameter for the unoxidized species. The isomer shift falls in the range for covalently bonded divalent iron.[23] From the course of the isomer shifts it is clear that the oxidation of Fe($SnB_{11}H_{11}$)(triphos) by iodine only proceeds at the tin atoms, while iron remains in the divalent state. The poor resolution of the $^{57}$Fe spectra is the result of the small iron content of both compounds. Nevertheless, the spectra allow for an assignment of the oxidation state.

**Discussion of the Electron-Counting Scheme.** It is well-known that the addition of further donor ligands to the skeleton of a *closo*-heteroborane leads to cage opening of the cluster. The addition of donors L or $X^-$ to *closo*-azaboranes $RNB_{11}H_{11}$ (R = H, Me, Ph) to give the nido species $RNB_{11}H_{11}L$ or $[RNB_{11}H_{11}X]^-$ is a prime example.[24] The phenylated *ortho*-disilaborane $(PhSi)_2B_{10}H_{10}$ forms the cage-opened intermediate $(PhSi)(MePhSi)B_{10}H_{10}$ upon treat-

(23) Wagner, F. E. Mössbauerspektroskopie. In *Untersuchungsmethoden in der Chemie*, 2nd ed.; Naumer, H., Heller, W., Eds.; Thieme: Stuttgart, Germany, 1990.
(24) Paetzold, P.; Müller, J.; Meyer, F.; Lomme, P. *Pure Appl. Chem.* **2003**, *75*, 1255−1261.

**Table 3.** Electron Count of $[I_2SnB_{11}H_{11}]^{2-}$

| vertex | contribution | total |
|---|---|---|
| 11 × BH | 2 | 22 |
| SnI | 3 | 3 |
| I | 1 | 1 |
| charge −2 | 2 | 2 |
| | | 28 cluster electrons |

ment with MeMgBr.[25] Further examples for cage-opening reactions which are of relevance in the context of this work are the reactions of neutral *closo*-stannacarbaboranes $Sn(CR)_2B_4H_4$,[26] $Sn(CMe)_2B_9H_9$,[27] and $Sn(CR)_2B_{10}H_{10}$[28,29] with Lewis bases to form heteroborane cages with slipped tin vertices whose structures do neither correspond to a classical closo or nido structures.

The structures of the iodinated clusters **1** and **3** can unequivocally be regarded as closo structures. The electron count corresponds to a nido count however (Table 3). According to the equation set up by Wade, the number of framework electron contributions by a main group element vertex is equal to $v + x - 2$ where $v$ is the number of valence-shell electrons and $x$ is the number of electrons from ligands ($x = 1$ for anionic ligands such as H, Me, Cl, and $x = 2$ for neutral Lewis bases like amines, pyridine, etc.). It is important to note that **1** and **3** formally have the same electron count as $(thf)Sn(CMe)_2B_9H_9$ which exhibits a significant displacement of the tin vertex from the center of the pentagonal carbollid face resulting from the electron donation to the tin center.[27] Jutzi and co-workers described the slippage of the tin vertex as a $\eta^5$ to $\eta^3$ rearrangement of the carbollid ligand which is similar to the distortion of the $[(C_5Me_5)Sn]^+$ fragment upon reaction with 2,2′-bipyridine.[30] The retention of a closo structure despite the addition of additional donor ligands is not unprecedented, and a related representative for such a behavior is the diethylamido adduct of the methylated *ortho*-silaborane $[1,2\text{-}\mu\text{-}(NEt_2)\text{-}1,2\text{-}(Me)_2\text{-}(Si_2B_{10}H_{10})]^-$ which maintains a closo structure but has an arachno electron count.[9]

The instability of **1** at room temperature suggests that the electronic situation of the cluster is not favorable. The decomposition products could not be identified unequivocally. However, the appearance of only one boron signal at −15.9 ppm in the $^{11}B\{^1H\}$ NMR spectrum excludes the formation of a nido species.

## Experimental Section

**General Methods.** All manipulations were carried out under dry argon in Schlenk glassware; solvents were dried and purified by standard methods and stored under argon. Elemental analyses were performed by the Institut für Anorganische Chemie, Universität Tübingen, using a Vario EL Analysator. Chemicals were purchased commercially except for $[Bu_3MeN]_2[SnB_{11}H_{11}]$[17] and $Fe(SnB_{11}H_{11})$(triphos),[13] which were prepared according to literature methods.

**Preparation of $[Bu_3MeN]_2[I_2SnB_{11}H_{11}]$ (1).** A solution of 129.9 mg (0.2 mmol) of $[Bu_3MeN]_2[SnB_{11}H_{11}]$ in 20 mL of $CH_2Cl_2$ was cooled to −78 °C, and 50.8 mg (0.2 mmol) of solid iodine was added. The solution became red immediately. Crystallization was carried out by layering the cooled $CH_2Cl_2$ solution with hexane in a Schlenk tube which was kept in a refrigerator at −35 °C for 5 days. The red single-crystals obtained decompose when kept at room temperature. $^{11}B$ NMR (acetone-$d_6$, −30 °C): $\delta$ −15.3 (5B), −17.2 (1B), −18.2 (5B). $^{119}Sn\{^1H\}$ NMR (acetone-$d_6$, −30 °C): $\delta$ −1039 (fwhh 560 Hz).

**Preparation of $Fe(I_2SnB_{11}H_{11})$(triphos) (3).** A solution of 50.8 mg (0.2 mmol) of $I_2$ in 5 mL of $CH_2Cl_2$ was added to a stirred solution of 185.8 mg (0.2 mmol) of $Fe(SnB_{11}H_{11})$(triphos) in 10 mL of $CH_2Cl_2$. After 5 min, a brown precipitate had formed and was collected via filtration. Yield: 177.5 mg, 75%. Single crystals suitable for X-ray analysis were grown by carefully layering an acetonitrile solution of $[Fe(SnB_{11}H_{11})(triphos)]$ with a solution of an equimolar amount of iodine in diethylether. $^1H$ NMR (DMSO-$d_6$): $\delta$ 6.7−7.3 (m, 30H, $C_6H_5$), 2.58 (m, 6H, $CH_2$), 1.81 (m, 3H, $CH_3$), −10.58 (br, 1H, B−H−Fe), −10.94 (br, 2H, B−H−Fe). $^{11}B$ NMR (DMSO-$d_6$): $\delta$ −13.0 to −25.0 (extremely broad), −31.0, −38.7. $^{31}P\{^1H\}$ NMR (DMSO-$d_6$): $\delta$ 53.2 ($A_2B$, 1P, $^2J(P,P)$ = 55.7 Hz), 51.2 ($A_2B$, 2P, $^2J(P,P)$ = 55.7 Hz). $^{119}Sn\{^1H\}$ NMR (DMSO-$d_6$, room temp): $\delta$ −749 (fwhh 1080 Hz). Elemental analaysis calcd. (%) for $C_{41}H_{50}B_{11}FeI_2P_3Sn$: C, 41.62; H, 4.26; I, 21.45. Found: C, 41.33; H, 4.01; I, 21.11.

**NMR Spectroscopy.** NMR spectra were obtained using a Bruker DRX-250 NMR spectrometer equipped with a 5 mm ATM probe head operating at 250.13 ($^1H$), 80.25 ($^{11}B$), 101.25 ($^{31}P$), and 93.25 MHz ($^{119}Sn$). Chemical shifts are reported in $\delta$ values relative to external TMS ($^1H$), $BF_3{\cdot}Et_2O$ ($^{11}B$), 85% aq $H_3PO_4$ ($^{31}P$), and $SnMe_4$ ($^{119}Sn$) using the chemical shift of the respective solvent $^2H$ resonance frequency.

**X-ray Structure Determination.** X-ray data for compounds **1** and **3** were collected on a Stoe IPDS2T and were corrected for Lorentz and polarization effects and absorption by air. A numerical absorption correction based on crystal-shape optimization was applied for all data. The programs used in this work are Stoe's X-Area including X-Red and X-Shape for data reduction and absorption correction[31] and the WinGX suite of programs[32] including SHELXS[33] and SHELXL[34] for structure solution and refinement.

**$[Bu_3MeN]_2[I_2SnB_{11}H_{11}]$ (1).** Two butyl chains of one tributylmethylammonium cation including C19−C22 and C23−C26 showed disorder over two positions with occupancies of 50.4:49.6 (C19−C22) and 52.3:47.7 (C23−C26). The disordered alkyl chains were refined with isotropic displacement parameters, and DFIX restraints were applied for all carbon carbon interatomic distances. All hydrogen atoms were kept at calculated positions.

**$Fe(I_2SnB_{11}H_{11})$(triphos)·$2CH_3CN$ (3).** All hydrogen atoms except the hydrogen atoms of the stannaborate cluster were placed in calculated positions and refined with isotropic displacement parameters. The B−H hydrogen atoms were located on difference maps and allowed to refine freely.


(25) Wesemann, L.; Trinkaus, M.; Englert, U.; Müller, J. *Organometallics* **1999**, *18*, 4654−4659.
(26) Saxena, A. K.; Maguire, J. A.; Hosmane, N. S. *Chem. Rev.* **1997**, *97*, 2421−2461.
(27) Jutzi, P.; Galow, P.; Abu-Orabi, S.; Arif, A. M.; Cowley, A. H.; Norman, N. C. *Organometallics* **1987**, *6*, 1024−1031.
(28) Wilson, N. M. M.; Ellis, D.; Boyd, A. S. F.; Giles, B. T.; Macgregor, S. A.; Rosair, G. M.; Welch, A. J. *Chem. Commun.* **2002**, 464−465.
(29) Wong, K. H.; Chan, H. S.; Xie, Z. *Organometallics* **2003**, *22*, 1775−1778.
(30) Kohl, F. X.; Schlüter, E.; Jutzi, P.; Krüger, C.; Wolmershäuser, G.; Hofmann, P.; Stauffert, P. *Chem. Ber.* **1984**, *117*, 1178−1193.
(31) *X-AREA 1.26;* Stoe und Cie GmbH: Darmstadt, Germany, 2005.
(32) Farrugia, L. J. *J. Appl. Crystallogr.* **1999**, *32*, 837−838.
(33) Sheldrick, G. M. *SHELXS-97, Program for the Solution of Crystal Structures*; Universität Göttingen: Göttingen, Germany, 1997.
(34) Sheldrick, G. M. *SHELXL-97, Program for Crystal Structure Refinement*; Universität Göttingen: Göttingen, Germany, 1997.

**$^{57}$Fe and $^{119}$Sn Mössbauer Spectroscopy.** A $^{57}$Co/Rh and a $Ca^{119m}SnO_3$ source were available for the $^{119}$Sn Mössbauer spectroscopic investigations. The samples were placed within thin-walled glass containers at a thickness of about 10 mg Sn(Fe)/cm$^2$. In the case of the $^{119}$Sn measurements, a palladium foil of 0.05 mm thickness was used to reduce the tin K X-rays concurrently emitted by this source. The measurements were conducted in the usual transmission geometry at 78 K.

**Acknowledgment.** This work was financially supported by the Deutsche Forschungsgemeinschaft.

**Supporting Information Available:** Crystallographic data in CIF format. This material is available free of charge via the Internet at http://pubs.acs.org.

IC0622858